J. Fluid Mech. (2003), *vol.* 496, *pp.* 295–312.
DOI: 10.1017/S0022112003006372 Printed in the United Kingdom

Stability analysis of a shear flow with strongly stratified viscosity

By PATRICIA ERN[1], FRANÇOIS CHARRU[1] AND PAOLO LUCHINI[2]

[1]Institut de Mécanique des Fluides, UMR CNRS/UPS-INP 5502, Allée du Professeur Camille Soula, 31400 Toulouse, France

[2]Dipartimento di Ingegneria Meccanica, Università di Salerno, 84084 Fisciano (SA), Italy

(Received 19 July 2002 and in revised form 22 April 2003)

A linear stability analysis of a shear flow in the presence of a continuous but steep variation of viscosity between two layers of nearly uniform viscosity is presented. This instability is investigated in relation to the known interfacial instability for the parallel flow of two superposed fluids of different viscosity. With respect to this configuration, the stability of our problem depends on two new parameters: the interface thickness δ and the Péclet number Pe, which accounts for diffusion effects when viscosity perturbations, coupled to the velocity perturbations, are allowed. We show that instability still exists for the continuous viscosity profile, provided the thickness of the interface is small enough and Pe sufficiently large. Small and large wavenumbers are found to be stable, at variance with the discontinuous configuration. Of particular interest is also the possibility of obtaining higher growth rates than in the discontinuous case for suitable Pe and δ ranges.

1. Introduction

Hydrodynamical shear instabilities in the presence of continuous viscosity stratification are widely encountered, for instance in many chemical engineering processes (like polymer extrusion or separation processes like filtration). Viscosity stratification is present in a flow when different fluids or temperature or concentration gradients are involved. Most fundamental studies have considered specifically the stability of channel flow in the presence of heating at the walls. In their comprehensive review, Wall & Wilson (1996) report in particular how the stability of plane Poiseuille flow is modified by temperature for four viscosity models. They found that viscosity stratification can have a significant influence on the stability of the flow. When the applied temperature gradient leads to a non-uniform increase of the viscosity everywhere in the channel, the flow is stabilized; if however it leads to a non-uniform decrease, the flow is either stabilized or destabilized. They highlight three main effects to explain this behaviour: a bulk effect due to the uniform increase or decrease of viscosity, a velocity-profile shape effect as the basic-state velocity profile becomes non-symmetrical, and a thin-layer effect when a thin layer of lower or higher viscosity develops adjacent to a channel wall. They also find that the stability of the flow is only weakly dependent on the value of the Péclet number Pe, which compares inertial and thermal diffusive effects. A companion paper (Wall & Wilson 1997) is devoted to boundary-layer flow stability over a heated or cooled plate. For the viscosity models considered, they find that when the applied temperature leads to a

non-uniform decrease (increase) of the viscosity towards the plate, the flow is stabilized (destabilized), a behaviour enhanced when the Prandtl number, which compares viscous and thermal diffusive effects, is increased. Ranganathan & Govindarajan (2001) also consider the high-Reynolds-number stability of plane channel flow but in the case of two fluids of different viscosities with a mixed layer in between. Unlike Wall & Wilson (1996, 1997), their analysis neglects any disturbance to the viscosity distribution; in order to be able to do so they assume $Pe = 0$ as far as perturbations are concerned, disregarding the fact that, if $Pe = 0$, the base flow diffuses instantaneously and therefore cannot retain the assumed viscosity stratification. In the context of non-Newtonian fluids and in the absence of diffusion effects ($Pe = \infty$), Wilson & Rallison (1999) have investigated the stability of elastic liquids having continuously stratified constitutive properties, in connection with the two-fluid co-extrusion instability that arises when elasticity varies discontinuously. They found that an Oldroyd-B fluid having a sufficiently rapid normal-stress variation is unstable. As a modified White–Metzner fluid having identical velocity and stress profiles is stable, they pointed out that Lagrangian convection of material properties (either polymer concentration or relaxation time) appears as a crucial ingredient of their instability.

In parallel to a continuous viscosity stratification, the case of discontinuous stratification has also sparked much interest. Indeed, when two superposed immiscible fluids of constant viscosity are sheared, an interfacial mode of instability arises depending on the thickness and viscosity ratio between the fluid layers and on the surface tension and gravity effects. Two major features of this instability are that it is triggered by an inertial effect, however small it may be, and that short as well as long wavelengths may become unstable (Yih 1967; Hooper & Boyd 1983). The mechanisms of instability for these wavelengths have been identified by Hinch (1984) and Charru & Hinch (2000). An interesting property is that when the thinner layer is the more viscous, the flow is unstable, whereas it is stable otherwise. In particular, a Couette-type shear flow in the presence of a thin and more viscous layer is known to be unstable and is well-documented. For instance, Albert & Charru (2000) provide the stability diagram in the plane of the parameters m and d, which respectively denote the viscosity and thickness ratio between the fluid layers, in the absence of surface tension and gravity effects. Throughout the present paper, this configuration will be termed 'the discontinuous case', as the viscosity and hence the slope of the velocity profile are discontinuous at the interface. Our concern in this work is with the existence and the characteristics of this interfacial mode of instability in the presence of a continuous stratification of viscosity.

The shear instability of a flow having a continuous and locally strong stratification of viscosity is relevant to some experiments with miscible fluids and resuspension flows. Several experiments have been devoted to the dynamics of miscible fluids displacing each other in pipes. When a less viscous fluid displaces a more viscous fluid in a tube, a fingering instability is known to occur (Petitjeans & Maxworthy 1996). The more viscous fluid is not totally displaced: it leaves a thin layer on the pipe wall that surrounds the finger as it travels. For certain flow rates and viscosity ratios, Scoffoni, Lajeunesse & Homsy (2001) reported that the finger shape exhibits a periodic axisymmetric or non-axisymmetric pattern. The Péclet number, Pe, of their experiment is large and the fluids appear to be well separated; thus, to explain their observations, they draw an analogy with the core–annular instability known to occur between immiscible fluids (Bai, Chen & Joseph 1992 and companion papers). The converse situation of a more viscous fluid displacing a less viscous fluid in a cylindrical tube was studied recently by Balasubramaniam, Rashidnia & Maxworthy

(2001). In this case too, not only fingering was observed to occur, but under certain conditions the advancing finger was observed to describe a sinuous pattern, as also happens for immiscible fluids (Joseph & Renardy 1993). However, though the discontinuous immiscible-fluid interfacial instability is a good candidate to explain these observations, the effect of diffusion on this instability, even at large Pe, and of a blurred interface, in which viscosity varies sharply but continuously, is unknown. These questions also arise in the case of resuspension flows. When a bed of small particles settled by gravity is sheared by the fluid flow, non-uniformities in the height of the bed and ripple growth have been observed to occur, hinting at the presence of instabilities (Schaflinger, Acrivos & Stibi 1995). The concentration profile in the resuspended layer may be obtained by balancing sedimentation due to gravity and particle diffusion due to the concentration gradient (Schaflinger, Acrivos & Zhang 1990; Leighton & Acrivos 1986). Since the resulting particle concentration in the flowing suspension is almost uniform except within a thin transition layer underneath the clear fluid, Zhang, Acrivos & Schaflinger (1992) performed a stability analysis of the problem by considering the suspension to have uniform physical properties. A question then arises about the effect on this instability of taking into account not only the real continuous variation of the concentration, and in particular the existence of a transition layer, but also the existence of concentration perturbations subject to diffusion, just as the base flow. In a first attempt to clarify these points, the purpose of the present paper is to characterize the effect of diffusion and of a blurred interface upon the interfacial mode of instability, known to exist at the interface between two superposed constant-viscosity fluids subject to shear. As detailed in the next section, the linear stability problem is then governed by two coupled equations: an Orr–Sommerfeld equation (momentum and mass conservation equations) with additional terms due to the continuous variation of the base flow viscosity and to the existence of viscosity perturbations, and a transport-diffusion equation governing temperature or concentration perturbations, together with a constitutive equation for viscosity versus temperature or concentration.

2. Governing equations

2.1. *Base flow*

We consider a base flow of constant density ρ and continuously varying viscosity μ_B. The coordinate x denotes the direction parallel and y perpendicular to the walls, which are located at $y = 0$ and $y = h_1 + h_2$. As shown on figure 1(a), the base flow viscosity μ_B is assumed to vary according to the law

$$\mu_B(y) = \mu_i + \Delta\mu \ \tanh\left(\frac{2}{\delta}\left(\frac{y}{h_1} - 1\right)\right) \tag{2.1}$$

$$\text{with} \quad \mu_i = \frac{\mu_1 + \mu_2}{2} \quad \text{and} \quad \Delta\mu = \frac{\mu_2 - \mu_1}{2}.$$

The dimensionless parameter δ is the representative thickness of the smoothed mixing layer around $y = h_1$ where most of the adjustment between the values μ_1 and μ_2 takes place. In the limit $\delta \to 0$, the discontinuous case is recovered with $\mu_B = \mu_1$ in a layer of thickness h_1 and $\mu_B = \mu_2$ in a layer of thickness h_2. A zero pressure gradient is assumed and the corresponding base flow velocity $(U_B(y), 0)$ is given by the momentum conservation equation

$$\frac{\mathrm{d}}{\mathrm{d}y}\left(\mu_B(y)\frac{\mathrm{d}U_B}{\mathrm{d}y}\right) = 0 \tag{2.2}$$

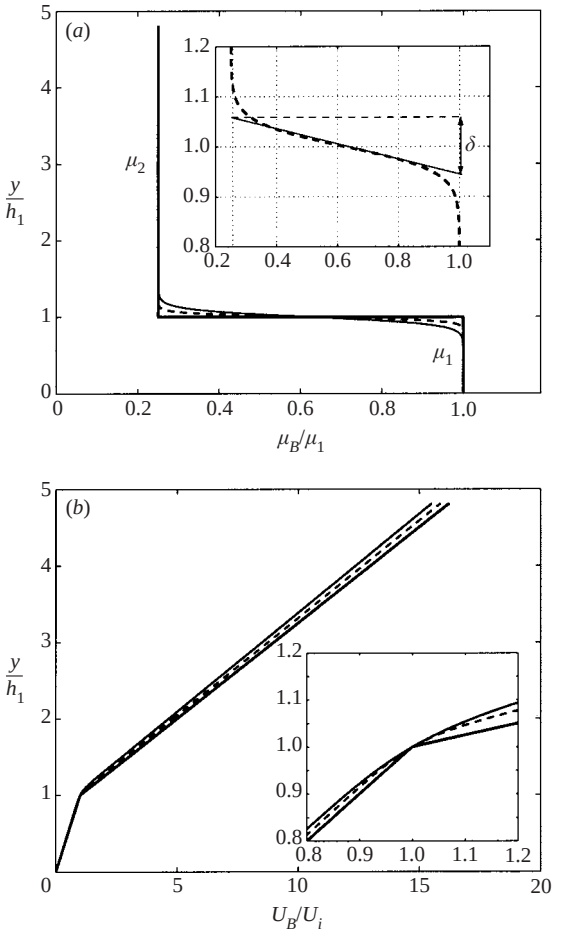

FIGURE 1. Base flow profiles of (a) the viscosity and (b) the velocity, for different values of δ, the mixing layer thickness: $\delta = 0.2$ (more rounded profile), $\delta = 0.1$ (dashed line) and $\delta = 0.002$ (sharper profile) ($\mu_2/\mu_1 = 0.25$, $h_2/h_1 = 4$).

with boundary conditions $U_B(0) = 0$ and $U_B(h_1) = U_i$. This equation is solved numerically and typical profiles of this Couette-type flow are shown in figure 1(b). For the purpose of non-dimensionalization, we choose as reference scales those of the thinner and more viscous layer identified by the subscript 1: h_1 as the length scale, μ_1 as the reference viscosity and $U_i = U_B(h_1)$ as the velocity scale. The Reynolds number Re and the Péclet number Pe then are

$$Re = \frac{\rho U_i h_1}{\mu_1} \quad \text{and} \quad Pe = \frac{U_i h_1}{D},$$

where D is a constant diffusion coefficient. We also define the parameters

$$d = \frac{h_2}{h_1} \quad \text{and} \quad m = \frac{\mu_2}{\mu_1}$$

and denote the non-dimensional base-flow velocity and viscosity as

$$U(y) = \frac{U_B}{U_i} \quad \text{and} \quad N(y) = \frac{\mu_B}{\mu_1}.$$

The viscosity μ is assumed to depend on an intensive quantity Φ, for instance a concentration or a temperature, which follows a transport-diffusion equation. For the sake of simplicity, we assume that the dependence of the viscosity on this quantity is linear in the required range

$$\mu(\Phi) = \lambda_0 \Phi + \mu_0, \tag{2.3}$$

λ_0 and μ_0 being constants, which will turn out to disappear in the stability equations. Note that Einstein's law for dilute suspensions corresponds to the case $\lambda_0 = (5/2)\,\mu_0$. The viscosity perturbation is then proportional to the Φ perturbation and follows the same transport-diffusion equation with velocity $\boldsymbol{U}$ and constant diffusion coefficient D:

$$\frac{\partial \mu}{\partial t} + (\boldsymbol{U} \cdot \nabla)\mu = \nabla \cdot (D \nabla \mu), \tag{2.4}$$

where ∇ is a gradient operator. It can be noticed that equation (2.4) is satisfied whatever the law $\mu(\Phi)$ when $Pe = \infty$ ($D = 0$), the viscosity becoming just a convectively transported scalar quantity. It should also be noted that the unperturbed base-flow viscosity profile (2.1) satisfies the above equation as a steady solution in the limit of zero diffusion only, $Pe = \infty$. As $Pe \gg 1$ and Re is finite in the cases studied here, we shall assume diffusion to be negligible as far as the base flow is concerned. This assumption becomes unacceptable if the growth rate of the disturbances is slower than the rate of change of the base state, that is, if the time scale of the disturbance growth is larger than the diffusion time scale of the interface thickness, $Pe\ \delta^2$. The limitations entailed by this condition will be discussed in more detail in § 3.5.

2.2. *Stability equations*

The linear stability analysis of the base flow $(U(y), 0)$ associated with the base viscosity $N(y)$ is performed by introducing in the Navier–Stokes, continuity and viscosity transport-diffusion equations the velocity perturbations $(u(y), v(y))\mathrm{e}^{\mathrm{i}(\alpha x - \omega t)}$ and the viscosity perturbation $n(y)\mathrm{e}^{\mathrm{i}(\alpha x - \omega t)}$, α being a dimensionless wavenumber and ω a dimensionless frequency. After linearization, these equations may then be recast in a similar form as in Wall & Wilson (1996), namely as the following coupled equations for $v(y)$ and $n(y)$:

$$\begin{aligned}(-\mathrm{i}\omega + \mathrm{i}\alpha U)\left(\frac{\mathrm{d}^2 v}{\mathrm{d}y^2} - \alpha^2 v\right) - \mathrm{i}\alpha \frac{\mathrm{d}^2 U}{\mathrm{d}y^2} v - \alpha^2 \frac{1}{Re}\left(\frac{\mathrm{d}^2 N}{\mathrm{d}y^2} + \alpha^2 N\right) \\ + 2\alpha^2 \frac{1}{Re}\frac{\mathrm{d}}{\mathrm{d}y}\left(N \frac{\mathrm{d}v}{\mathrm{d}y}\right) - \frac{1}{Re}\frac{\mathrm{d}^2}{\mathrm{d}y^2}\left(N \frac{\mathrm{d}^2 v}{\mathrm{d}y^2}\right) + \mathrm{i}\alpha \frac{1}{Re}\left(\frac{\mathrm{d}^2}{\mathrm{d}y^2} + \alpha^2\right)\left(n \frac{\mathrm{d}U}{\mathrm{d}y}\right) = 0,\end{aligned} \tag{2.5}$$

$$(-\mathrm{i}\omega + \mathrm{i}\alpha U)n + v \frac{\mathrm{d}N}{\mathrm{d}y} - \frac{1}{Pe}\left(\frac{\mathrm{d}^2 n}{\mathrm{d}y^2} - \alpha^2 n\right) = 0, \tag{2.6}$$

with the boundary conditions $v = \mathrm{d}v/\mathrm{d}y = n = 0$ at $y = 0$ and $y = 1 + d$. The velocity perturbation u is then given by the continuity equation $\mathrm{i}\alpha u + \mathrm{d}v/\mathrm{d}y = 0$. The classical Orr–Sommerfeld equation is recovered for N constant and $n = 0$.

A second-order-accurate finite-difference discretization is used. Discretization points are more tightly spaced in the interface region: for instance 165 grid points within the transition layer compared to 400 points in the whole channel. The eigenvalue problem for the resulting linear system of algebraic equations is solved numerically for a real α and complex $\omega = \omega_r + \mathrm{i}\omega_i$. The results were verified by repeating the computation for different discretization steps and found repeatable within graphical accuracy except for a region of very small diffusivity or very small

thickness of the mixing layer where the true solution or its derivatives become discontinuous and the precision of the discretization is degraded. The difference between the growth rate found for 1000 grid points and that found for 2000 grid points is typically less than 10^{-5}.

2.3. *The limit of infinite Péclet number*

The limit of infinite Péclet number ($D = 0$) and finite Re is particularly interesting because in this limit the base flow does not diffuse at all and the assumption of an arbitrary viscosity profile being steady becomes exact. However, there is a singularity for (2.5)–(2.6), as the order of the equations becomes reduced in this limit, which requires special treatment for a numerical solution to be found. That the system of (2.5)–(2.6) may lead, for $Pe = \infty$, to a singular solution can be seen by extracting v from (2.6), in the form

$$v = (\mathrm{d}N/\mathrm{d}y)^{-1}\mathrm{i}(\omega - \alpha U)n$$

and inserting it into (2.5). Once this is done, $(\omega - \alpha U)$ appears in the coefficient of the highest (fourth) derivative, meaning that the solution may become singular at a position where this coefficient is zero. It should be noted by contrast that, if a similar substitution is performed for finite Péclet number, the highest derivative in the single resulting equation is the sixth, and its coefficient never becomes zero.

This behaviour is quite analogous to the infinite-Reynolds-number limit of the classical Orr–Sommerfeld equation governing the stability of a homogeneous fluid. Whereas for finite Reynolds number the highest (fourth) derivative has a constant non-zero coefficient, for infinite Reynolds number the highest (second) derivative in the resulting Rayleigh equation is multiplied by $(\omega - \alpha U)$. Although no singularity is thus introduced for general complex ω, the eigenfunction for the particularly interesting neutral case where the function $\omega(\alpha)$ crosses the real axis is characterized by a logarithmic singularity at the so-called critical layer, i.e. the value of y where $U(y) = \omega/\alpha$. From a numerical viewpoint, this circumstance makes the neutral point difficult to find.

A classical remedy in the context of the Rayleigh equation is to analytically continue the solution to a suitable path in complex y. In fact, by so doing the value of ω where ω/α crosses the curve $U = U(y)$ (supposedly a known analytical function) becomes complex, and the eigenfunction with ω real no longer entails a singularity. In other words, the solution at the neutral point is now computed along a complex path which turns around and stays away from its singularity located on the real axis, and along which it can be numerically discretized without any difficulty. From a programming viewpoint, doing this requires little more than declaring complex a number of variables that were real before, and assigning a suitable discrete path in the complex-y plane. The infinite-Pe results that will be presented below are obtained by this technique, with the use of a parabolic path connecting the two real positions of the channel's end walls. Of course, the numerical solutions have been verified to be independent of the actual path chosen, and to be identical (to within discretization error) with their real-y counterpart when ω is complex or Pe is finite.

3. Instability results

3.1. *Instability properties*

In this section, we investigate the effect of diffusion, through the Péclet number Pe, and of the interface thickness δ on the instability characteristics: the growth rate ω_i

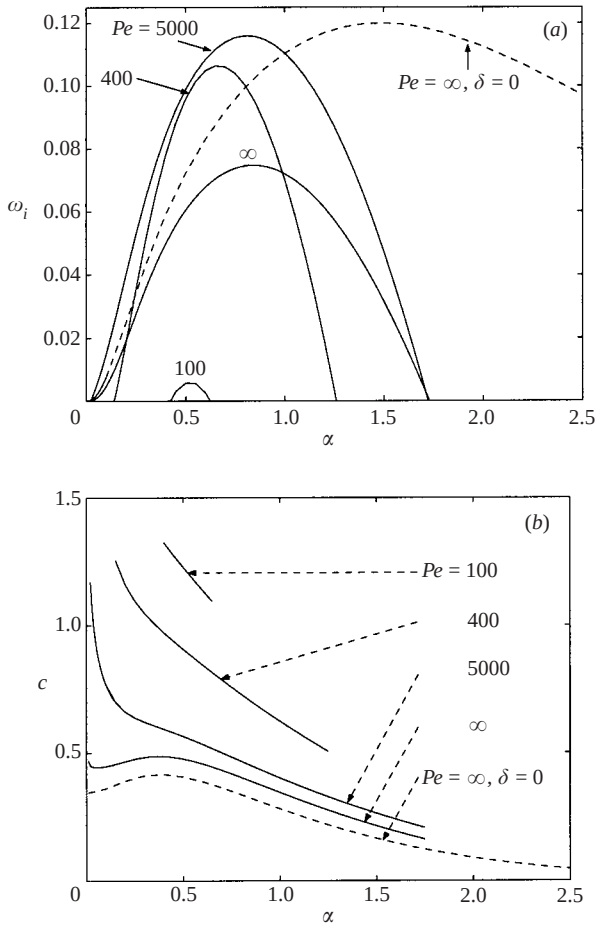

FIGURE 2. Evolution with the wavenumber α of (a) the growth rate ω_i and (b) the phase velocity c for $Pe = 100, 400, 5000$ and ∞, and for $\delta = 0.1$ ($Re = 0.25, m = 0.25$ and $d = 4$). The evolution for the discontinuous case ($Pe = \infty, \delta = 0$) is also drawn (dashed line).

and the phase velocity relative to the midpoint of the mixing layer, $c = \omega_r/\alpha - 1$. Unless otherwise stated, the other parameters are fixed at the values $Re = 0.25$, $m = 0.25$ and $d = 4$, for which the discontinuous two-layer Couette flow is known to be unstable (Albert & Charru 2000). The evolution of ω_i and c with α is presented in figure 2 for $\delta = 0.1$ and $Pe = 100,\ 400,\ 5000$ and ∞, showing that the interfacial mode of instability still exists in the presence of diffusion and of a blurred interface. Of particular interest is the fact that only a band of wavenumbers is unstable: small as well as large wavenumbers are found to be stable. This is at variance with the discontinuous case ($Pe = \infty, \delta = 0$), which is unstable for all wavenumbers, as shown on the same figure (dashed line). The curve $\omega_i(\alpha)$ has a sharper peak and its maximum is shifted towards lower wavenumbers. For some Pe values, wavenumbers $\alpha \simeq 0.5$ have a larger growth rate than in the discontinuous case. In the absence of diffusion ($D = 0$, $Pe = \infty$) but for a blurred interface ($\delta \neq 0$), stability of small and large wavenumbers is also observed, like in Wilson & Rallison (1999). Results for $Pe = 10^6$ (computed along a real path) are indistinguishable from those for $Pe = \infty$ (computed along a complex path) within graphical accuracy. Figure 2(b) shows for

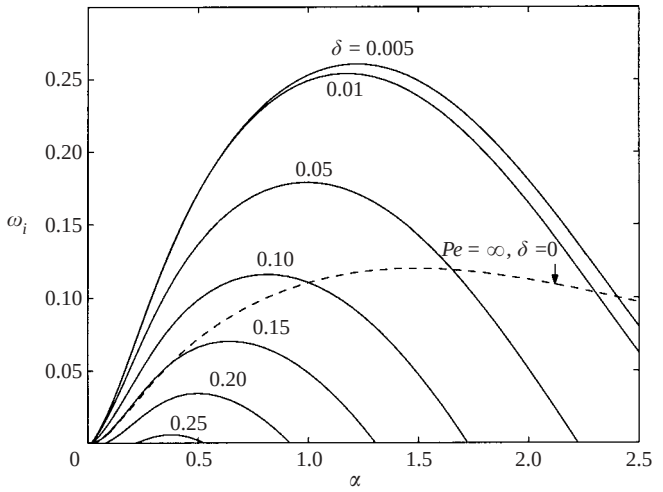

FIGURE 3. Evolution with the wavenumber α of the growth rate ω_i for several values of δ and for $Pe = 5000$ ($Re = 0.25$, $m = 0.25$ and $d = 4$). The evolution for the discontinuous case ($Pe = \infty$, $\delta = 0$) is also drawn (dashed line).

$Pe = 100$, 400 and 5000 a monotonic decrease of phase velocity c with wavenumber α, also at variance with the discontinuous case and the case $Pe = \infty$ where it increases before decreasing. When Pe decreases, c increases, as confirmed later in this paper.

The instability features are also strongly dependent on the interface thickness δ. Figure 3 shows the evolution of the growth rate ω_i with wavenumber α, for several values of the interface thickness δ and for $Pe = 5000$. The growth rate and the band of unstable wavenumbers are seen to increase as δ decreases. For $\delta \leqslant 0.01$, the curves nearly superpose, eventually corresponding to the extreme case $\delta = 0$. The evolution corresponding to the discontinuous case ($Pe = \infty$, $\delta = 0$) is also drawn for comparison. Noteworthy is the fact that a larger growth rate is obtained for $Pe = 5000$ and $\delta \leqslant 0.1$ than for the discontinuous case. A comparison between the modulus of the eigenfunction component u for the discontinuous case and for $Pe = 10^5$ is presented in figure 4. The eigenfunction for the discontinuous case is obtained for the wavenumber $\alpha = 10^{-3}$ using the analytical expansion at small wavenumbers given by Yih (1967). For $Pe = 10^5$, the eigenfunctions plotted also correspond to $\alpha = 10^{-3}$ and to interface thicknesses $\delta = 0.005$ and $\delta = 0.1$, as indicated in the figure.

3.2. *Order-of-magnitude considerations*

A tentative explanation of the effect of the Péclet number Pe on the flow stability at small and large wavenumbers can be obtained, following Hinch (1984), by comparing the diffusion time τ_D of the disturbance and the characteristic time for the inertial instability $\tau_I = 1/\omega_i$. The condition for instability is that there be little diffusion over a wavelength before the instability has grown , i.e. $\tau_D > \tau_I$. The time τ_I can be estimated by its value for the discontinuous case. For large wavenumbers, and provided $\delta \ll 1/\alpha$, τ_I and τ_D are (Hinch 1984)

$$\tau_I = \frac{\alpha^2 \nu_1}{{U_i}^2} \quad \text{and} \quad \tau_D = \frac{h_1^2}{\alpha^2 D} \tag{3.1}$$

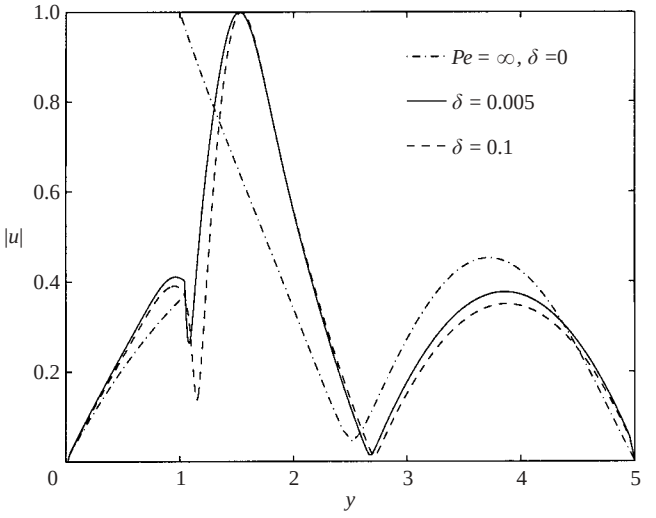

FIGURE 4. Comparison for $\alpha = 10^{-3}$ of the modulus of the eigenfunction component u for the discontinuous case (dash-dot line); for $Pe = 10^5$, $\delta = 0.005$ (solid line) and for $Pe = 10^5$, $\delta = 0.1$ (dashed line) ($Re = 0.25$, $m = 0.25$ and $d = 4$).

so that the condition is

$$\frac{Re\ Pe}{\alpha^4} > 1. \tag{3.2}$$

Thus, when Pe increases, the higher wavenumber that satisfies the condition also increases. For given large α and small Re, the Péclet number Pe has to be very large to have instability; equivalently, the smaller Pe is, the bigger Re must be. For $Pe = 400$ and $Re = 0.25$, condition (3.2) for instability is only fulfilled for $\alpha < 3.2$, which is consistent with figure 2.

At large wavelengths ($\alpha \ll 1$), $Re = O(1)$, $d \gg 1$, and provided $\delta \ll 1$, τ_I for the two-layer flow is (Charru & Hinch 2000)

$$\tau_I = \frac{60\ m^2}{(1-m)\ \alpha^2\ d^2\ Re}\ \frac{h_1}{U_1}. \tag{3.3}$$

With diffusion, the instability condition $\tau_D > \tau_I$ then gives

$$\frac{(1-m)}{m^2}\ \frac{Re\ Pe\ \alpha^2\ d^2}{60} > 1 \quad \text{for} \quad \tau_D = \frac{h_1^2}{D}. \tag{3.4}$$

Again, the product $Re\ Pe$ must be sufficiently large for an instability to be observed at small α. In the present case of small Re, this means that the diffusion must be weak enough. When Pe decreases, the smaller wavenumber that satisfies this condition increases. For $Pe = 400$ and $Re = 0.25$, condition (3.4) for instability requires $\alpha > 0.055$, which is consistent with figure 2.

3.3. *Interface thickness and diffusion effects*

The effect of diffusion and thickness of the interface on the range of unstable wavenumbers is now investigated numerically. Figure 5 presents the neutral curve in the plane α–Pe for several values of the interface thickness δ. The region inside each curve corresponds to the unstable wavenumbers for the indicated value of δ. For each value of δ, no wavenumber is unstable for Pe smaller than a critical value $Pe_c(\delta)$ (for example, $Pe_c = 68$ for $\delta = 0.005$). When δ increases, Pe_c increases.

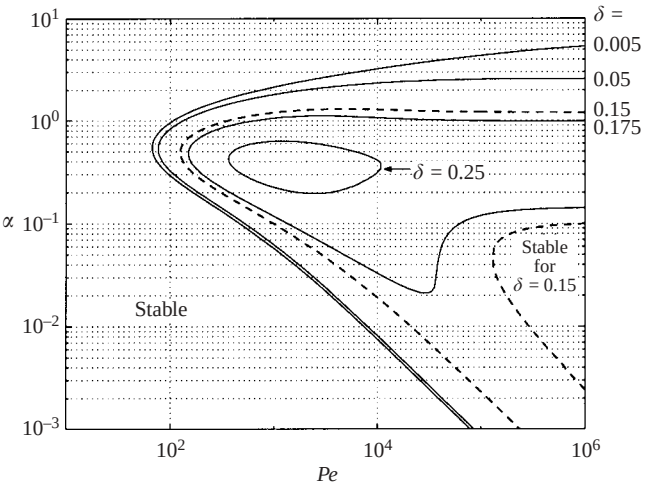

FIGURE 5. Neutral curve in the plane α–Pe for several values of the interface thickness δ ($Re = 0.25$, $m = 0.25$ and $d = 4$). Note that for $\delta = 0.15$ (dashed curve) there is a range of stable wavenumbers inside the range of unstable wavenumbers.

The associated critical wavenumber weakly depends on δ: $\alpha_c \simeq 0.5$. For $\delta = 0.15$ (dashed line), a region of stable wavenumbers exists at large Pe inside the band of unstable wavenumbers. When δ increases further, the two stable domains merge and the unstable domain shrinks, eventually becoming just a small island. Thus, for large δ, an instability is obtained only in a definite range of Pe. For $\delta = 0.005$, the largest unstable wavenumber, denoted α_L, increases with Pe, as expected from § 3.2, but not as $Pe^{1/4}$ (equation (3.2)). For $0.05 \leqslant \delta \leqslant 0.175$, α_L is nearly constant at large values of Pe ($Pe > 10^4$) and seems therefore to be selected by δ and not by Pe. Similarly, as expected from § 3.2, the smallest unstable wavenumber, say α_S, decreases with Pe but not as proposed by equation (3.4). The order of magnitude considerations of § 3.2 thus provide the qualitative tendencies of the evolution of the bounding unstable wavenumbers with Pe but not the correct scalings. The estimate of the effect of diffusion through a diffusion time only is probably oversimplified as the phase velocity is also affected.

The range of unstable wavenumbers also depends on the interface thickness δ, as illustrated in figure 6 which presents the neutral curve in the α–δ plane for several values of Pe. The region inside each curve corresponds to the unstable wavenumbers for the indicated value of Pe. As δ increases, the range of unstable wavenumbers shrinks. Wilson & Rallison (1999) also found that for a blurred concentration profile and in the absence of diffusion ($Pe = \infty$), small and large wavenumbers are stable, the range of unstable wavenumbers reducing as the thickness of the blurred interface increases. For $Pe < 1250$, the curves are of similar shape and for $0.005 \leqslant \delta \leqslant 0.03$, α_L and α_S vary only slightly with δ, which means that the cut-off of the range of unstable wavenumbers is mainly determined by Pe for these Pe and δ values. The curve for $Pe = 5000$ is much broader and the effect of δ on α_L and α_S is more important. Note that for $Pe = 1250$, instability exists for larger values of δ.

3.4. *Most amplified mode*

For given Pe, δ, Re, m and d, the growth rate ω_i is only a function of the wavenumber α. We shall denote its maximal value as $\omega_{i,max}$, the corresponding wavenumber α_{max}

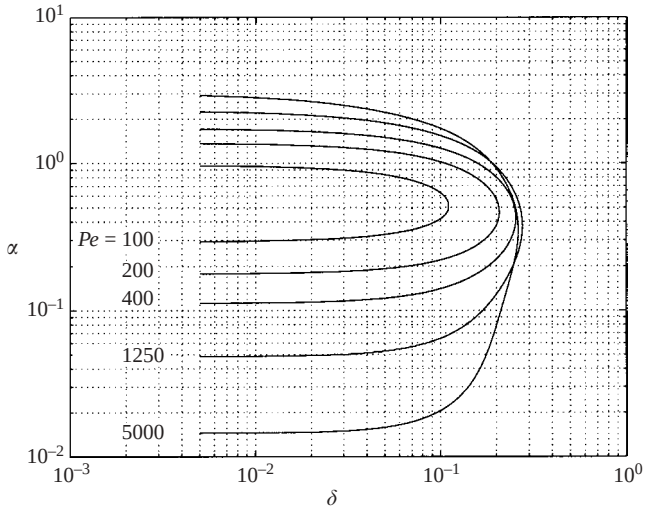

FIGURE 6. Neutral curve in the plane α–δ for several values of the Péclet number Pe ($Re = 0.25$, $m = 0.25$ and $d = 4$).

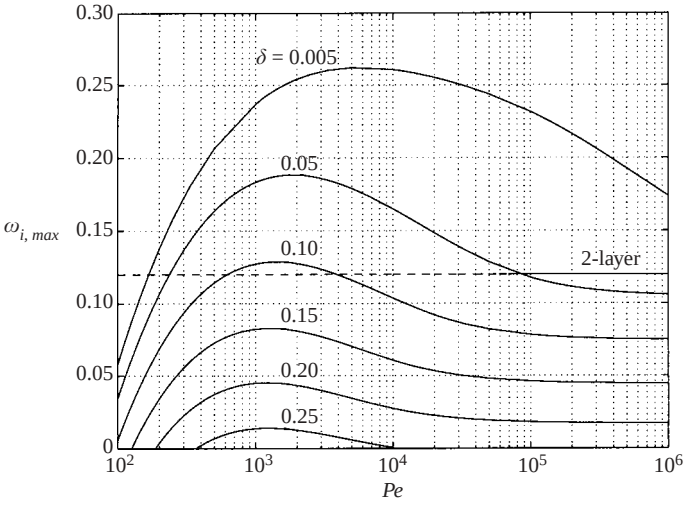

FIGURE 7. Maximum growth rate $\omega_{i,max}$ as function of Pe for several values of the interface thickness δ ($Re = 0.25$, $m = 0.25$ and $d = 4$). The horizontal dashed line $\omega_{i,max} = 0.12$ corresponds to the maximal value of the growth rate for the discontinuous two-layer flow ($Pe = \infty$, $\delta = 0$).

and phase velocity c_{max}. The effect of the Péclet number on this most amplified mode is now explored, the other parameters being kept fixed. Figure 7 displays the evolution of $\omega_{i,max}$ as a function of Pe for several values of δ. The value $\omega_{i,max} = 0.12$ corresponding to the discontinuous two-layer flow ($Pe = \infty$, $\delta = 0$) is also drawn. For large Pe ($Pe \geqslant 10^5$), $\omega_{i,max}$ depends only on δ for $\delta > 0.1$, with a value lower than in the discontinuous case. Whatever the interface thickness δ, decreasing Pe then has the rather unexpected effect of increasing the growth rate of the instability. The growth rate $\omega_{i,max}$ reaches a maximum for a particular value of Pe, which may be considered as an optimal diffusion for destabilizing the flow. This optimal value of

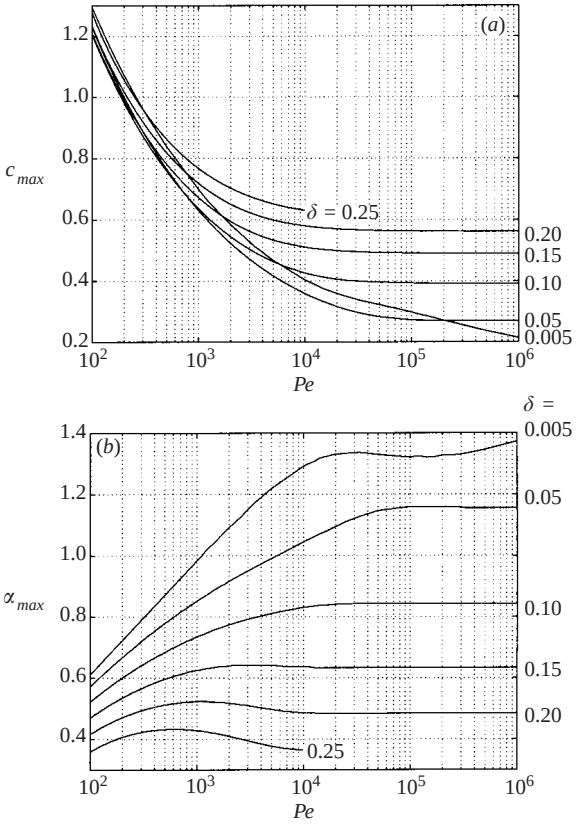

FIGURE 8. Evolution with Pe of (a) the phase velocity c_{max} associated with $\omega_{i,max}$ and (b) the wavenumber α_{max} for several values of the interface thickness δ ($Re = 0.25$, $m = 0.25$ and $d = 4$). For the discontinuous two-layer flow, $\alpha_{max} = 1.5$ and $c_{max} = 0.16$ associated with $\omega_{i,max} = 0.12$.

Pe increases only slightly when δ decreases for $\delta \geqslant 0.05$ (between $Pe = 1250$ and $Pe = 2500$). Of particular interest is the fact that the maximal growth rates obtained in the presence of diffusion for $\delta \leqslant 0.1$ are higher than in the discontinuous case. When Pe is decreased further, the growth rate $\omega_{i,max}$ decreases, eventually becoming negative. For the smallest values of Pe, $\omega_{i,max}$ decreases nearly linearly with δ. Figure 8 presents the evolution with Pe of the associated phase velocity c_{max} and wavenumber α_{max} for several values of δ. When Pe increases, the phase velocity c_{max} decreases, by a factor of 2 for the larger δ and of 4 for the smaller δ, before becoming constant for $Pe > 5000$ and $\delta \geqslant 0.1$. For the smaller Pe, c_{max} does not depend strongly on δ (less than 10%) but for $Pe \geqslant 10^5$, it grows by a factor of 3. Like $\omega_{i,max}$ and c_{max}, the wavenumber α_{max} depends on δ only and not on Pe, for $Pe \geqslant 5000$ and $\delta \geqslant 0.1$. For $Pe \leqslant 10^3$, α_{max} also depends almost linearly on δ, the slope increasing with Pe.

All the results presented up to now have been obtained for fixed values of the parameters m, d and Re, chosen such that an instability exists in the discontinuous case. The fact that for some Pe and δ the maximal growth rate is larger than for the two-layer flow allows us to expect that a stable discontinuous configuration may now also become unstable in the presence of diffusion and a blurred interface. This is indeed found to be the case. The results of Albert & Charru (2000) indicate that the

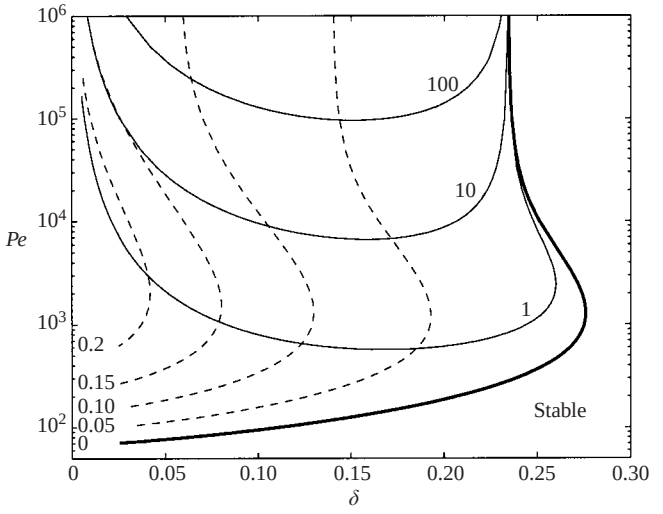

FIGURE 9. Isovalues of the maximum growth rate $\omega_{i,max}$ in the Pe–δ plane ($Re = 0.25$, $m = 0.25$ and $d = 4$): bold line: $\omega_{i,max} = 0$; dashed lines: $\omega_{i,max} = 0.05$, 0.1, 0.15 and 0.2. The curves labelled 1, 10 and 100 indicate the domain of the parameters where $\omega_{i,max}$ is respectively 1, 10 and 100 times larger than $Pe^{-1}\delta^{-2}$.

discontinuous case $d = 4$, $m = 2$ is stable for $\alpha = 0.1$ and 1 and unstable for $\alpha = 3$ and 10. In our configuration, calculations performed for $d = 4$, $m = 2$ and $Re = 0.25$ have shown that wavenumbers $\alpha \simeq 1$ are unstable for $10^4 < Pe < 10^5$ and $\delta = 0.02$, with growth rate $\omega_i \simeq 10^{-2}$ and phase velocity $c \simeq -0.1$. Note that this negative phase velocity is consistent with the result of Albert & Charru (2000) that waves move with the less viscous fluid.

3.5. *Base-flow diffusion*

Attention is now focused on the domain of existence of the instability in the Pe–δ plane. Isocontours of the maximal growth rate $\omega_{i,max}$ in the Pe–δ plane are shown in figure 9 for $Re = 0.25$, $m = 0.25$ and $d = 4$. The marginal linear stability curve is given by the contour $\omega_{i,max} = 0$. The region on the right of this curve corresponds to stable flow conditions. In the region on the left of the curve, at least one wavenumber is unstable, showing that the two-layer Couette flow with continuous variation of the viscosity exhibits instability provided the thickness of the mixing layer is small enough and the Péclet number Pe sufficiently large. Note that, for the largest thicknesses $0.25 \leqslant \delta \leqslant 0.276$, Pe must also not be too large for an instability to arise. Thus, for large interface thickness δ, only a range of Pe values provides an instability. There is also a particular value of Pe which destabilizes the largest interface thickness ($Pe = 1250$ for $\delta = 0.276$), which may be considered an optimal diffusion as discussed in the preceding section. Conversely, small interface thicknesses withstand a larger diffusion (smaller Pe). We found that the lower-branch values vary linearly with δ^{-1}. A notable feature of figure 9 is that the isovalue curves of $\omega_{i,max}$ are similar in shape, the largest growth rates being found for smaller values of δ, as already observed in figure 3.

As noted in § 2, we have neglected the diffusion of the base flow in our stability calculations. By physical reasoning, we may expect this approximation to become invalid if the diffusion of the base flow is faster than the growth of the normal modes.

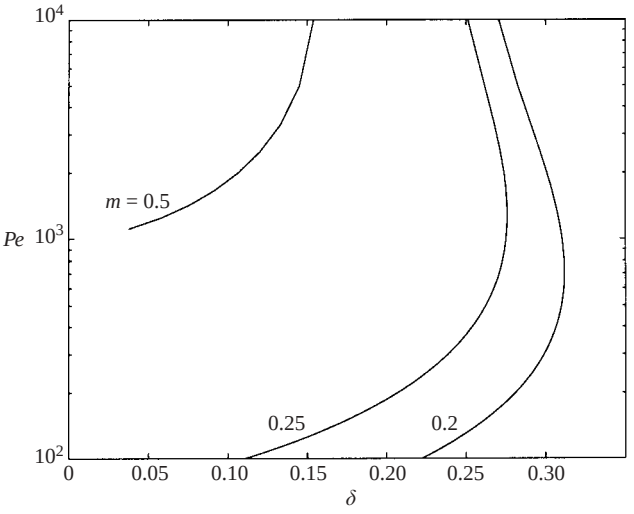

FIGURE 10. Marginal linear stability curves $\omega_{i,max} = 0$ in the Pe–δ plane for different viscosity ratios, the Reynolds number of the thicker and less viscous layer being kept fixed $Re_2 = 4$ and $d = 4$.

That is, this approximation may be expected to be inappropriate if the diffusion time scale of the base flow $\tau_{diff} = \delta^2/D$ is smaller than the characteristic time for instability $\tau_I = 1/\omega_i$. In non-dimensional form, for an instability to be observed we thus require that $\omega_i \gg Pe^{-1}\delta^{-2}$. The curves where $\omega_{i,max}$ is equal to 1, 10 and 100 times $Pe^{-1}\delta^{-2}$, drawn in figure 9, give an indication of how much smaller the diffusion of the base flow can be expected to be than the instability growth. We note that, since δ increases when base-flow diffusion prevails, the region on the left of each limiting curve may also be included in the corresponding instability domain, as instability will eventually prevail after diffusion makes δ large enough. It should also be noted, however, that base-flow diffusion completely rules out the case of zero Péclet number considered by Ranganathan & Govindarajan (2001).

3.6. *Some comments on the effect of other parameters*

The influence of the other parameters of the problem, $m = \mu_2/\mu_1$, $d = h_2/h_1$ and Re, has been thoroughly investigated in the discontinuous case (Albert & Charru 2000). In particular, the growth rate was found to be proportional to both Reynolds number and viscosity difference (and therefore zero when viscosities are equal). In this paper, we concentrated our attention on the influence of Pe and δ; the effect of other parameters can be expected to be qualitatively similar to the discontinuous case. This is illustrated in figure 10 where the neutral curve in the Pe–δ plane is plotted for three values of the viscosity ratio m and for the parameters $Re_2 = 4$ and $d = 4$, Re_2 being the Reynolds number of the thicker and less viscous layer. This figure indeed shows that increasing m reduces the instability domain. Now, however, the flow becomes unstable for $m < 0.85$ instead of 1 (Albert & Charru 2000). Similarly, the region where $\omega_{i,max} \gg Pe^{-1}\delta^{-2}$ is also considerably extended by decreasing the viscosity ratio m, as the growth rate becomes larger. Increasing Re has a similar effect on this region. The effect of the Reynolds number on the growth rate ω_i has also been explored in the range $0.001 \leqslant Re \leqslant 1000$, for four given wavenumbers ($\alpha = 0.5,\ 1,\ 1.5$ and 2) and the combinations of three values of Pe (100, 400, 5000) and three values of δ (0.05, 0.1, 0.15); the following trends were

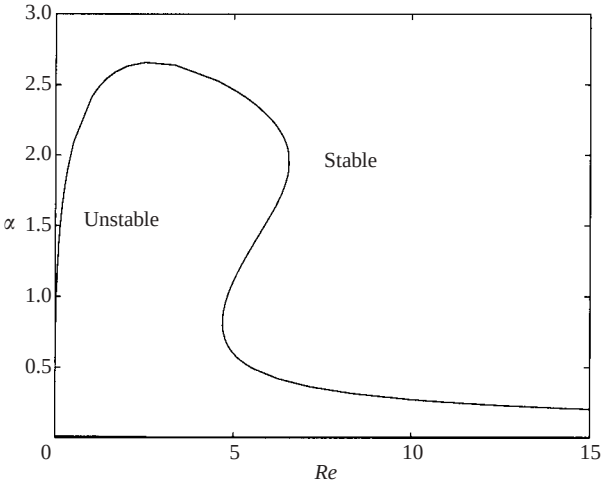

FIGURE 11. Marginal linear stability curve $\omega_i = 0$ in the plane α–Re for $Pe = 10^4$, $\delta = 0.1$, $m = 0.25$ and $d = 4$.

observed. In most cases, the instability only sets in above a critical Reynolds number $Re_{c1}(\alpha,\ \delta,\ Pe)$, at variance with the discontinuous case. When Re exceeds a second critical value $Re_{c2}(\alpha,\ \delta,\ Pe)$, the instability disappears, in agreement with the fact that, for the discontinuous case wavenumbers of order 1 stabilize when Re increases (Albert & Charru 2000). Decreasing Pe or increasing δ was found to increase the value of Re_{c1}. For the restabilization when Re increases, a decrease of Pe was observed to preserve the instability and therefore increase Re_{c2}, whereas increasing δ was found to stabilize the flow (Re_{c2} decreases). Figure 11 shows a typical example of the marginal linear stability curve in the plane α–Re for $Pe = 10^4$, $\delta = 0.1$, $m = 0.25$ and $d = 4$. The lower boundary of unstable wavenumbers, $\alpha_S < 0.015$, is indistinguishable from the Re-axis. For $Re > 6.6$, wavenumbers $\alpha \gtrsim 0.4$ are stable, whereas small wavenumbers remain unstable.

Finally, we have tested the sensitivity of the growth rate to the precise shape of the viscosity profile by trying laws other than the hyperbolic one. Calculations have been performed for a cosine viscosity distribution, matching the values of μ_1 and μ_2 as follows:

$$\mu_B(y) = \mu_i + \Delta\mu\ \sin\left(\frac{2}{\delta}\left(\frac{y}{h_1} - 1\right)\right) \quad \text{for} \quad h_1\left(1 - \tfrac{1}{4}\pi\delta\right) < y < h_1\left(1 + \tfrac{1}{4}\pi\delta\right)$$

as well as a piecewise linear viscosity distribution:

$$\mu_B(y) = \mu_i + \Delta\mu\ \frac{2}{\delta}\left(\frac{y}{h_1} - 1\right) \quad \text{for} \quad h_1\left(1 - \tfrac{1}{2}\delta\right) < y < h_1\left(1 + \tfrac{1}{2}\delta\right).$$

These profiles, just like the profile given by equation (2.1), have been defined to have the same slope at the midpoint of the interface, $y/h_1 = 1$. As shown on figure 12, the results of the calculations exhibit relatively small differences, in the range of what can be expected from the effective thickness of the region of rapid change of viscosity in the three profiles. Differences for the phase velocity are less than 10%. Our results are thus only weakly dependent on the specific viscosity distribution chosen to describe the transition layer.

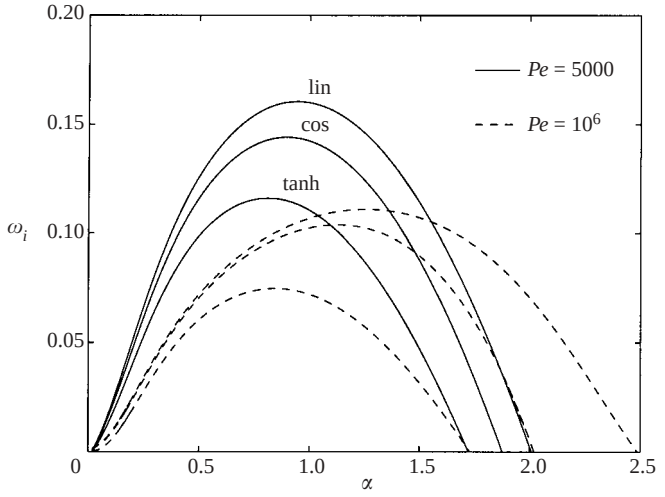

FIGURE 12. Evolution with the wavenumber α of the growth rate ω_i for three different base viscosity distributions describing the rapid change from one layer to the other: the hyperbolic tangent profile studied in this paper and a linear and a cosine distribution (for $\delta = 0.1$, $Pe = 5000$ and $Pe = 10^6$; and for $Re = 0.25$, $m = 0.25$, $d = 4$).

4. Conclusion

The linear stability of the continuous analogue to the two-layer Couette shear flow has been studied by considering a hyperbolic-tangent distribution of the base-flow viscosity. The analysis required us to account for the coupling between viscosity and velocity perturbations and for the effects of diffusion, i.e. of the Péclet number Pe, and of the interface thickness δ. Results show that instability still exists in the presence of diffusion and of a blurred interface, provided the thickness of the mixing layer δ is not too large and Pe is not too small. For the larger interface thicknesses ($0.25 \leqslant \delta \leqslant 0.276$ for $Re = 0.25$, $d = 4$ and $m = 0.25$), only a range of Péclet numbers Pe allows instability (roughly $400 \leqslant Pe \leqslant 10^4$). When Pe decreases ($70 < Pe < 400$), the largest interface thickness δ_c allowing instability decreases. This regime occurs for a wavenumber $\alpha \simeq 0.5$. However for these flow conditions, an instability is unlikely to be encountered in practice as the base flow may diffuse faster than the instability grows. Larger growth rates are found for smaller δ and larger Pe values, and are associated with larger wavenumbers ($\alpha \simeq 1$) and smaller phase velocities. The various instability regimes are more clearly seen when Pe and δ are varied independently. For the smaller unstable Pe, the maximal growth rate $\omega_{i,max}$ varies linearly with Pe and δ. The phase velocity c_{max} was shown to depend strongly on Pe whatever δ. For larger Pe values ($Pe > 2 \times 10^4$), on the contrary, $\omega_{i,max}$, α_{max} and c_{max} depend more strongly on δ than on Pe and eventually only on δ for $\delta > 0.1$. Between these two regimes, there is an optimal Pe value giving a maximal growth rate roughly independent of δ. Of particular interest is the fact that the growth rate is larger than the growth rate for the discontinuous case for a range of Pe and δ. Owing to this effect, a stable discontinuous configuration could be destabilized by diffusion. Calculations have indeed shown that some wavenumbers which are stable in a discontinuous case are destabilized in our configuration for a range of Pe and δ values. The domain of existence of the interfacial instability in the presence of diffusion and a thick interface is therefore modified in the plane of the parameters m and d with respect to the discontinuous configuration. One

of the most prominent features of this instability is however the fact that only a band of wavenumbers is unstable whatever Pe or δ, whereas long and short wavelengths are found to be stable. This is at variance with the discontinuous configuration, which is known to be unstable for all wavenumbers. The band of unstable wavenumbers reduces as δ increases, but the behaviour with Pe is more complex, depending on the value of δ. It appears that, although order-of-magnitude considerations may explain the stability of large and small wavenumbers in the presence of diffusion, the smallest and largest unstable wavenumbers are strongly dependent on δ, for large Pe.

Thus, the presence of diffusion and of a blurred interface does not cancel the interfacial mode of instability, known to exist at the interface between two superposed fluids subjected to shear, but in some cases even enhances it. Our results therefore support the possibility that this instability could be a good candidate to explain the experimental observations on miscible fluids and resuspension flows mentioned in the Introduction. In our case, however, the domain of existence of this instability depends strongly on the governing parameters and the range of unstable wavenumbers is found to be reduced. At this stage, the level of agreement with the available experiments is difficult to assess. From the pictures presented by Scoffoni *et al.* (2001), it seems that their instability has a wavelength much larger than both the viscous-film thickness and the finger size. The density contrast between their fluids ranges from 0.05% to 11% and the viscosity ratio is $10 < m < 400$. The Péclet number is large, $Pe \sim 10^5$–10^6. In the case of resuspension flows, Schaflinger *et al.* (1995) reported that the observed waves have a wavelength comparable to the total spacing of the duct, which is twice the height of the suspension layer. A weak-amplitude wave of wavelength about twenty times the total spacing was also observed. From their theoretical base flow profile, one might guess a thickness of their interface smaller than 0.05. In both cases, a quantitative comparison could only be performed if measurements were available of the base velocity and viscosity profiles as well as of the interface thickness, in order to perform our stability calculations for the appropriate base-flow distribution, viscosity–concentration relationship and governing parameters.

REFERENCES

Albert, F. & Charru, F. 2000 Small Reynolds-number instabilities in two-layer Couette flow. *Eur. J. Mech.* B *Fluids* **19**, 229–252.

Bai, R., Chen, K. & Joseph, D. 1992 Lubricated pipelining: stability of core-annular flow. Part 5. Experiments and comparison with theory. *J. Fluid Mech.* **240**, 97–132.

Balasubramaniam, R., Rashidnia, N. & Maxworthy, T. 2001 Instability of miscible interfaces in a cylindrical tube. In *Proc. 1st Intl Workshop on Miscible Interfaces, ESPCI, Paris, France.*

Charru, F. & Hinch, J. 2000 "Phase diagram" of interfacial instabilities in a two-layer Couette flow and mechanism of the long-wave instability. *J. Fluid Mech.* **414**, 195–223.

Hinch, J. 1984 A note on the mechanism of the instability at the interface between two shearing fluids. *J. Fluid Mech.* **144**, 463–465.

Hooper, A. & Boyd, W. 1983 Shear-flow instability at the interface between two viscous fluids. *J. Fluid Mech.* **128**, 507–528.

Joseph, D. & Renardy, Y. 1993 *Fundamentals of Two-fluids Dynamics*. Springer.

Leighton, D. & Acrivos, A. 1986 Viscous resuspension. *Chem. Engng Sci.* **41**, 1377–1384.

Petitjeans, P. & Maxworthy, T. 1996 Miscible displacements in capillary tubes. Part 1: Experiments. *J. Fluid Mech.* **326**, 37–56.

Ranganathan, B. & Govindarajan, R. 2001 Stabilization and destabilization of channel flow by location of viscosity-stratified fluid layer. *Phys. Fluids* **13**, 1–3.

Schaflinger, U., Acrivos, A. & Stibi, H. 1995 An experimental study of viscous resuspension in a pressure-driven plane channel flow. *Intl J. Multiphase Flow* **21**, 693–704.

Schaflinger, U., Acrivos, A. & Zhang, K. 1990 Viscous resuspension of a sediment within a laminar and stratified flow. *Intl J. Multiphase Flow* **16**, 567–578.

Scoffoni, J., Lajeunesse, E. & Homsy, G. 2001 Interface instabilities during displacements of two miscible fluids in a vertical pipe. *Phys. Fluids* **13**, 552–556.

Wall, D. & Wilson, S. 1996 The linear stability of channel flow of fluid with temperature-dependent viscosity. *J. Fluid Mech.* **323**, 107–132.

Wall, D. & Wilson, S. 1997 The linear stability of flat-plate boundary-layer of fluid with temperature-dependent viscosity. *Phys. Fluids* **9**, 2885–2898.

Wilson, H. & Rallison, J. 1999 Instability of channel flows of elastic liquids having continuously stratified properties. *J. Non-Newtonian Fluid Mech.* **85**, 273–298.

Yih, C. 1967 Instability due to viscous stratification. *J. Fluid Mech.* **27**, 337–352.

Zhang, K., Acrivos, A. & Schaflinger, U. 1992 Stability in a two-dimensional Hagen–Poiseuille resuspension flow. *Intl J. Multiphase Flow* **18**, 51–63.